

# Micro- and Macrostructural magneto-electric coupling in soft composites

Matthias Rambašek<sup>1\*</sup> and Marc-André Keip<sup>1</sup>

## Micro Abstract

It was only recently that strong magneto-electric coupling effects in soft-matter-based composites have been described for the first time by Liu and Sharma (2013; Phys. Rev. E 88, 040601). This approach for the realization of magneto-electrical coupling has the potential to outperform existing solutions based on ceramic materials. In this contribution we will investigate magneto-electric transducers based on a soft magneto-electric composite with multiscale simulations.

<sup>1</sup>Institute of Applied Mechanics (CE), University of Stuttgart, Stuttgart, Germany

\*Corresponding author: matthias.rambašek@mechbau.uni-stuttgart.de

## Introduction

More than a decade ago, the works [5, 17] (re-)initiated research on magneto-electrically coupling materials. Motivated by these findings, continuum-mechanical approaches to magneto-electric coupling based on multiscale methods have been developed [9, 10, 15]. The research in these references focuses on the magneto-electric coupling properties of ferroic composites based on hard constituents. However, only recently, an alternative route to magneto-electric coupling with focus on new types of magnetic-field sensors has been proposed [11]. The magneto-electric coupling described in [11] differs from earlier approaches by its reliance on macroscopic effects.

Inspired by the above works, we strive for a deeper understanding of macroscopic magneto-electric coupling effects. For this purpose we extend our previous work on magnetorheological elastomers [6, 7] to the domain of magneto-electro-elasticity. Since magnetorheological elastomers (MREs) do not only have magneto-mechanical but also electro-mechanical coupling properties, all properties needed for the macroscopic magneto-electric coupling are at hand. Furthermore, it is known that the magneto-mechanical response of MREs strongly depends on their microstructure [2, 6] such that their micromorphology has a strong impact on their macroscopic magneto-electric coupling performance.

In this contribution we present multiscale simulations of MRE bodies under homogeneous external magnetic and electric fields in a two-dimensional setting. Thereby we focus on the magneto-electric coupling relevant for magnetic-field sensors.

## Theory

In the quasi-static setting under consideration in absence of free currents, the governing (Maxwell) equations for the electric and magnetic fields are given as

$$\operatorname{div} \mathbf{d} = q, \quad \operatorname{div} \mathbf{b} = 0, \quad \operatorname{curl} \mathbf{e} = \mathbf{0} \quad \text{and} \quad \operatorname{curl} \mathbf{h} = \mathbf{0}, \quad (1)$$

where  $\mathbf{d}$  is the electric displacement,  $q$  the free electric charge density,  $\mathbf{b}$  the magnetic induction,  $\mathbf{e}$  the electric field and  $\mathbf{h}$  the magnetic field [8]. Furthermore, we introduce the polarization  $\mathbf{p}$  and the magnetization  $\mathbf{m}$  via the relations

$$\mathbf{d} = \varepsilon_0 \mathbf{e} + \mathbf{p} \quad \text{and} \quad \mathbf{h} = \frac{\mathbf{b}}{\mu_0} - \mathbf{m}. \quad (2)$$

Finally, we have jump conditions which in absence of surface charges and currents read as

$$[[\mathbf{d}]] \cdot \mathbf{n} = 0, \quad [[\mathbf{b}]] \cdot \mathbf{n} = 0, \quad [[\mathbf{e}]] \times \mathbf{n} = \mathbf{0} \quad \text{and} \quad [[\mathbf{h}]] \times \mathbf{n} = \mathbf{0}. \quad (3)$$

Regarding the governing equations for mechanics, we employ the concept of the total first-Piola-Kirchhoff-type stress  $\mathbf{P}^{tot}$  [3, 4], which captures purely mechanical, magneto- and electro-mechanical stresses. The kinematic quantity dual to  $\mathbf{P}^{tot}$  is the deformation gradient  $\mathbf{F}$ . The corresponding equations then are

$$\text{Div} \mathbf{P}^{tot} = -\mathbf{f}_0^b \quad \text{and} \quad \text{Curl} \mathbf{F} = \mathbf{0}, \quad (4)$$

where  $\mathbf{f}_0^b$  is the mechanical body force per referential volume. At this point we want to note that the lowercase differential operators  $\{\text{div}, \text{grad}, \text{curl}\}$  as employed in (1) refer to derivatives with respect to Eulerian coordinates  $\mathbf{x}$  of the current configuration. Conversely, their uppercase counterparts  $\{\text{Div}, \text{Grad}, \text{Curl}\}$  denote derivatives with respect to Lagrangian coordinates  $\mathbf{X}$  of the initial configuration. The relation between the current and the initial configuration is described in terms of the deformation map  $\varphi$  from which we also define  $\mathbf{F}$

$$\mathbf{x} = \varphi(\mathbf{X}) \quad \text{and} \quad \mathbf{F} = \text{Grad} \varphi \quad (5)$$

such that (4)<sub>2</sub> is fulfilled identically. For the description of incompressible media the Cauchy stress is decomposed into a deviatoric part  $\text{dev}[\boldsymbol{\sigma}^{tot}]$  and a volumetric part  $-p^{tot}\mathbf{1}$ , where  $p^{tot}$  can be shown to be the Lagrange multiplier enforcing the kinematic constraint of incompressibility [1]. The relevant jump conditions for  $\mathbf{P}^{tot}$  and  $\mathbf{F}$  are given as

$$[[\mathbf{P}^{tot}]] \cdot \mathbf{N} = \mathbf{t}^{mech} \quad \text{and} \quad [[\mathbf{F}]] \times \mathbf{N} = \mathbf{0}, \quad (6)$$

with the mechanical traction  $\mathbf{t}^{mech}$ .

### Constitutive relations

In this contribution, we employ an energy-based formulation. In case of magneto-electro-elasticity this means that we consider Helmholtz-free-energy densities parametrized as follows

$$\psi(\mathbf{C}, \mathbf{d}, \mathbf{b}) \quad \text{and} \quad \Psi(\mathbf{F}, \mathbf{D}, \mathbf{B}) = \psi(\mathbf{F}^T \cdot \mathbf{F}, \frac{1}{J} \mathbf{F} \cdot \mathbf{D}, \frac{1}{J} \mathbf{F} \cdot \mathbf{B}), \quad (7)$$

where  $\mathbf{C} = \mathbf{F}^T \cdot \mathbf{F}$  and  $\{\mathbf{D}, \mathbf{B}\}$  are the referential counterparts of  $\{\mathbf{d}, \mathbf{b}\}$ . In the case of incompressibility, we introduce the energy density [1, 14]

$$\Psi^*(\mathbf{F}, \mathbf{D}, \mathbf{B}) = \Psi(\mathbf{F}^*, \mathbf{D}, \mathbf{B}) = \psi((\mathbf{F}^*)^T \cdot \mathbf{F}^*, \mathbf{F}^* \cdot \mathbf{D}, \mathbf{F}^* \cdot \mathbf{B}). \quad (8)$$

Therein,  $\mathbf{F}^* = \frac{1}{J^{1/dim}} \mathbf{F}$  with  $dim = \text{tr} \mathbf{1}$  is the isochoric part of the deformation gradient. Furthermore, we have

$$\{\mathbf{P}, \mathbf{E}, \mathbf{H}\} = \left\{ \frac{\partial \Psi}{\partial \mathbf{F}}, \frac{\partial \Psi}{\partial \mathbf{D}}, \frac{\partial \Psi}{\partial \mathbf{B}} \right\} \quad \text{and} \quad \{\mathbf{P}^*, \mathbf{E}, \mathbf{H}\} = \left\{ \frac{\partial \Psi^*}{\partial \mathbf{F}}, \frac{\partial \Psi^*}{\partial \mathbf{D}}, \frac{\partial \Psi^*}{\partial \mathbf{B}} \right\} \quad (9a)$$

for compressible and incompressible media, respectively.

### Variational principle on the macroscopic scale

In the macroscopic setting we want to consider the presence of free charge densities  $q$ . This motivates us to employ  $\varphi$ ,  $\mathbf{D}$  and  $\mathbf{B}$  as primary fields. This choice means that we have to explicitly account for the balance equations

$$\text{Div} \mathbf{P} = -\mathbf{f}_0^b, \quad \text{Div} \mathbf{D} = q_0, \quad \text{and} \quad \text{Div} \mathbf{B} = 0. \quad (10)$$

The corresponding functional is the below Lagrangian function with multipliers  $\phi^e$ ,  $\phi^m$  and  $p^{\text{tot}}$

$$\begin{aligned} \mathcal{L}(\boldsymbol{\varphi}, \mathbf{D}, \mathbf{B}, p^{\text{tot}}, \phi^e, \phi^m) &= \int_{\mathcal{B}} \Psi^*(\mathbf{F}, \mathbf{D}, \mathbf{B}; \mathbf{X}) + p^{\text{tot}}(J - 1) \, dV + \int_{\Omega \setminus \mathcal{B} = \mathcal{B}'} \Psi(\mathbf{F}, \mathbf{D}, \mathbf{B}; \mathbf{X}) \, dV \\ &+ \int_{\Omega} -\phi^e(\text{Div} \mathbf{D} - q_0(\mathbf{X})) - \phi^m(\text{Div} \mathbf{B}) \, dV + \Pi^{\text{ext}}, \end{aligned} \quad (11)$$

where  $\mathcal{B}$  is the domain occupied by the body in the referential configuration,  $\Omega$  denotes the whole domain consisting of  $\mathcal{B}$  and the surrounding free space  $\mathcal{B}'$  [6].  $\Pi^{\text{ext}}$  refers to external loading. Thus, we obtain the variational saddle-point principle

$$\left\{ \hat{\boldsymbol{\varphi}}, \hat{\mathbf{D}}, \hat{\mathbf{B}}, \hat{p}^{\text{tot}}, \hat{\phi}^e, \hat{\phi}^m \right\} = \arg \left\{ \inf_{\substack{\boldsymbol{\varphi} \\ \in \mathcal{W}_{\boldsymbol{\varphi}}}} \inf_{\substack{\mathbf{D} \\ \in \mathcal{W}_{\mathbf{D}}}} \inf_{\substack{\mathbf{B} \\ \in \mathcal{W}_{\mathbf{B}}}} \sup_{\substack{p^{\text{tot}} \\ \in \mathcal{W}_p}} \sup_{\substack{\phi^e \\ \in \mathcal{W}_{\phi^e}}} \sup_{\substack{\phi^m \\ \in \mathcal{W}_{\phi^m}}} \mathcal{L}(\boldsymbol{\varphi}, \mathbf{D}, \mathbf{B}, p^{\text{tot}}, \phi^e, \phi^m) \right\}. \quad (12)$$

### Variational principle on the microscopic scale and homogenization

At the microscale, we do not consider the case of free charge densities such that we may resort to a formulation of magneto-electro-elasticity [13] in terms of electric and magnetic vector potentials  $\mathbf{A}^e$  and  $\mathbf{A}^m$ , respectively. Then the electric displacement and the magnetic induction fields are obtained as  $\mathbf{D} = \text{Curl} \mathbf{A}^e$  and  $\mathbf{B} = \text{Curl} \mathbf{A}^m$ . Hence, the balance equations (10)<sub>2-3</sub> are fulfilled identically.

In this work we employ the FE<sup>2</sup>-method [12] to account for micro-heterogeneity of the MRE body  $\mathcal{B}$ . Accordingly, we introduce the macroscopic energy density of the referential volume element  $(\mathcal{RVE}) \mathcal{B}[\bar{\mathbf{X}}]$  at  $\bar{\mathbf{X}}$ , following [13],

$$\bar{\Psi}^*(\bar{\mathbf{F}}, \bar{\mathbf{D}}, \bar{\mathbf{B}}) = \inf_{\substack{\boldsymbol{\varphi} \\ \in \mathcal{W}_{\boldsymbol{\varphi}}(\bar{\mathbf{F}})}} \inf_{\substack{\mathbf{A}^e \\ \in \mathcal{W}_{\mathbf{A}^e}(\bar{\mathbf{D}})}} \inf_{\substack{\mathbf{A}^m \\ \in \mathcal{W}_{\mathbf{A}^m}(\bar{\mathbf{B}})}} \sup_{\substack{p^{\text{tot}} \\ \in \mathcal{W}_p}} \int_{\mathcal{B}[\bar{\mathbf{X}}]} \Psi^*(\mathbf{F}^*, \mathbf{D}, \mathbf{B}) + p^{\text{tot}}(J - 1) \, dV. \quad (13)$$

For details on the appropriate spaces  $\mathcal{W}_{\boldsymbol{\varphi}}$ ,  $\mathcal{W}_{\mathbf{A}^e}$ ,  $\mathcal{W}_{\mathbf{A}^m}$  we refer to [13,16]. Furthermore, we force the average pressure to zero. The macroscopic constitutive quantities are obtained as

$$\bar{\mathbf{P}}^* = \frac{1}{|\mathcal{B}_{\bar{\mathbf{X}}}|} \int_{\partial \mathcal{B}[\bar{\mathbf{X}}]} (\mathbf{P}^* \cdot \mathbf{N}) \otimes \mathbf{X} \, dA \quad \text{and} \quad \{\bar{\mathbf{E}}, \bar{\mathbf{H}}\} = \frac{1}{|\mathcal{B}_{\bar{\mathbf{X}}}|} \int_{\partial \mathcal{B}[\bar{\mathbf{X}}]} (\{\mathbf{E}, \mathbf{H}\} \cdot \mathbf{X}) \mathbf{N} \, dA. \quad (14a)$$

### Numerical Example

We consider a square two-dimensional MRE specimen with compliant electrodes attached at the top and bottom edges, which are employed to polarize the MRE specimen. Additionally, the MRE is exposed to a homogeneous external magnetic field as depicted in Figure 1. The Helmholtz-free-energy function we employ for incompressible media is

$$\psi = \frac{\mu}{2} (\mathbf{F}^* : \mathbf{F}^* - 3) + \frac{1}{2\epsilon_0} \|\mathbf{d}\|^2 - \frac{1}{2\epsilon_0} \frac{\chi^e}{J + \chi^e} \|\mathbf{d}\|^2 + \frac{1}{2\mu_0} \|\mathbf{b}\|^2 - \frac{m^{\text{sat}}}{\gamma} \ln [\cosh(\gamma \|\mathbf{b}\|)] \quad (15)$$

with  $\gamma = J\chi^m/(m^{\text{sat}}(J + \chi^m))$ . The material parameters for the elastomer matrix are set to  $\{\mu, \chi^e, m^{\text{sat}}, \chi^m\} = \{0.06667, 7, 0, 0\}$  and to  $\{\mu, \chi^e, m^{\text{sat}}/\sqrt{\mu_0}, \chi^m\} = \{66.67, 700, 1, 10\}$  for the inclusions. For the electrodes on the macroscopic scale we use  $\{\mu, \chi^e, m^{\text{sat}}, \chi^m\} = \{0.6667, 10^5, 0, 0\}$ . The free space on the macroscopic scale is modeled with  $\{\mu, \chi^e, m^{\text{sat}}, \chi^m\} = \{0.001, 0, 0, 0\}$ , whereby the mechanical term in (15) is replaced by a compressible neo-Hookean energy density with  $\lambda = 0$  [6]. The constants  $\epsilon_0$  and  $\mu_0$  are set to  $8.854 \times 10^{-6}$  and  $0.4\pi$ , respectively.

In Figure 2 we depict the sensitivity of the electric field  $\mathbf{e}^s$  detected by a sensor (see Figure 1) with respect to the external magnetic field  $\mathbf{b}^\infty$ . There we also see the influence of the applied

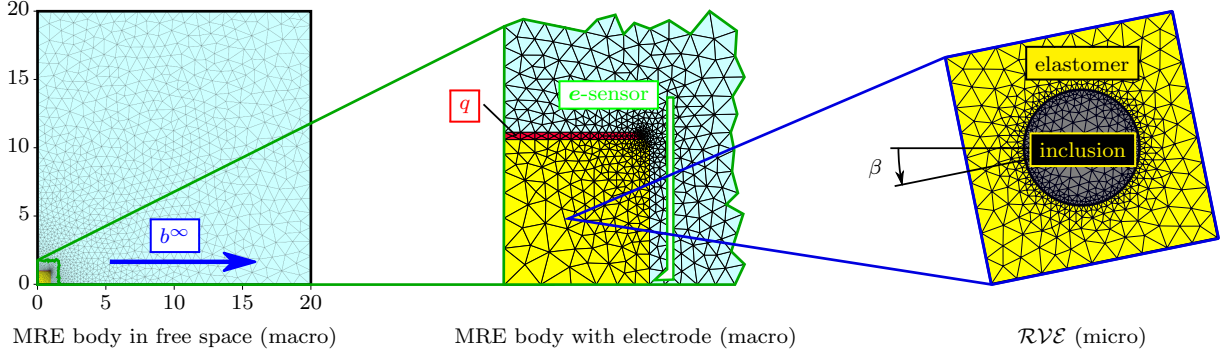


**Figure 1.** The square MRE specimen is embedded into a sufficiently sized free space with homogeneous external magnetic field  $\mathbf{b}^\infty$  (left). In the zoomed view of the specimen we indicate the electric loading via charge density  $q$  and the location of the electric field sensor. The microscopic  $\mathcal{RVE}$  is depicted at the very right.

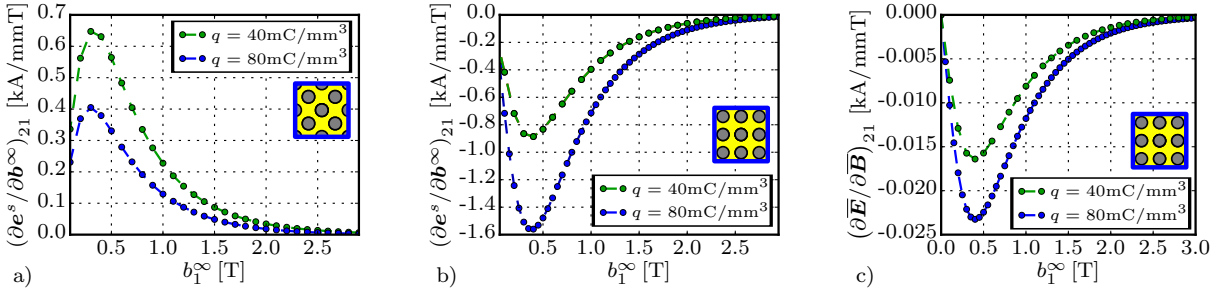


**Figure 2.** In a) we show the sensitivity of the detectable electric field at the specimen scale for a microstructure with angle  $\beta = \pi/4$ . Interestingly, the peak sensitivity is achieved for  $q = 40\text{mC}/\text{mm}^3$ . In b) we show the same graph for the case of  $\beta = 0$ , where the magnitude of the sensitivity is maximal for the  $q = 80\text{mC}/\text{mm}^3$ -curve. Obviously, the corresponding effective magneto-electric modulus depicted in c) is orders of magnitude smaller.

electric free charge density in the electrodes. Additionally, we also investigate the effect of the microstructure orientation. Next to the characteristic sensor property we show the corresponding material modulus, which obviously does not play a significant role.

## Conclusions

In this contribution we investigated the performance of MREs as magnetic-field sensors in a two-dimensional setting. With our multiscale simulations we confirm the analytical observations in [11] regarding the performance of such devices. We conclude that for the example under consideration, the macrostructural magneto-electric effects [11] dominate. The underlying magneto- and electro-mechanical properties, however, are governed by the MRE microstructure.

## Acknowledgements

The financial support of the German Research Foundation (DFG) in the Research Group 1509 “Ferroic Functional Materials” (project KE 1849/2-2) and the framework of the Cluster of Excellence in “Simulation Technology” (EXC 310/2) at the University of Stuttgart and as well as of the *Ministerium für Wissenschaft, Forschung und Kunst des Landes Baden-Württemberg* is gratefully acknowledged.

## References

- [1] J. Bonet and R. D. Wood. *Nonlinear continuum mechanics for finite element analysis*. Cambridge University Press, Cambridge, UK; New York, 2nd edition, 2008.
- [2] K. Danas. Effective response of classical, auxetic and chiral magnetoelastic materials by use of a new variational principle. *Journal of the Mechanics and Physics of Solids*, 105:25 – 53, 2017.
- [3] A. Dorfmann and R. W. Ogden. Magnetoelastic modelling of elastomers. *European Journal of Mechanics-A/Solids*, 22:497–507, 2003.
- [4] A. Dorfmann and R. W. Ogden. Nonlinear electroelasticity. *Acta Mechanica*, 174(3):167–183, 2005.
- [5] W. Eerenstein, N. D. Mathur, and J. F. Scott. Multiferroic and magnetoelectric materials. *Nature*, 442(7104):759–765, 2006.
- [6] M.-A. Keip and M. Rambašek. A multiscale approach to the computational characterization of magnetorheological elastomers. *International Journal for Numerical Methods in Engineering*, 107(4):338–360, 2016.
- [7] M.-A. Keip and M. Rambašek. Computational and analytical investigations of shape effects in the experimental characterization of magnetorheological elastomers. *International Journal of Solids and Structures*, 121:1–20, 2017.
- [8] A. Kovetz. *Electromagnetic Theory*. Oxford University Press, Oxford, 2000.
- [9] M. Labusch, M. Etier, D. C. Lupascu, J. Schröder, and M.-A. Keip. Product properties of a two-phase magneto-electric composite: Synthesis and numerical modeling. *Computational Mechanics*, 54:71–83, 2014.
- [10] J. Lee, J. G. Boyd, and D. C. Lagoudas. Effective properties of three-phase electro-magneto-elastic composites. *International Journal of Engineering Science*, 43(10):790–825, 2005.
- [11] L. Liu and P. Sharma. Giant and universal magnetoelectric coupling in soft materials and concomitant ramifications for materials science and biology. *Physical Review E*, 88(4):040601, 2013.
- [12] C. Miehe, J. Schotte, and J. Schröder. Computational micro-macro transitions and overall moduli in the analysis of polycrystals at large strains. *Computational Materials Science*, 16:372–382, 1999.
- [13] C. Miehe, D. Vallicotti, and S. Teichtmeister. Homogenization and multiscale stability analysis in finite magneto-electro-elasticity. Application to soft matter EE, ME and MEE composites. *Computer Methods in Applied Mechanics and Engineering*, 300:294–346, 2016.
- [14] J.-P. Pelteret, D. Davydov, A. McBride, D. K. Vu, and P. Steinmann. Computational electro- and magneto-elasticity for quasi-incompressible media immersed in free space. *International Journal for Numerical Methods in Engineering*, 108(11):1307–1342, 2016.
- [15] J. Schröder, M. Labusch, and M.-A. Keip. Algorithmic two-scale transition for magneto-electro-mechanically coupled problems: FE<sup>2</sup>-scheme: Localization and homogenization. *Computer Methods in Applied Mechanics and Engineering*, 302:253–280, 2016.
- [16] A. S. Semenov, H. Kessler, A. Liskowsky, and H. Balke. On a vector potential formulation for 3d electromechanical finite element analysis. *Communications in Numerical Methods in Engineering*, 22(5):357–375, 2006.
- [17] N. A. Spaldin and M. Fiebig. The Renaissance of Magnetoelectric Multiferroics. *Science*, 309(5733):391–392, 2005.